crystals

MDPI

Article

Effect of Fineness and Heat Treatment on the Pozzolanic Activity of Natural Volcanic Ash for Its Utilization as Supplementary Cementitious Materials

Kaffayatullah Khan [1,*], Muhammad Nasir Amin [1,*], Muhammad Usman [2], Muhammad Imran [3], Majdi Adel Al-Faiad [4] and Faisal I. Shalabi [1]

1 Department of Civil and Environmental Engineering, College of Engineering, King Faisal University (KFU), P.O. Box 380, Al-Hofuf, Al-Ahsa 31982, Saudi Arabia; fshalabi@kfu.edu.sa
2 Interdisciplinary Research Center for Hydrogen and Energy Storage (IRC-HES), King Fahd University of Petroleum & Minerals (KFUPM), Dhahran, Eastern Province 31261, Saudi Arabia; muhammadu@kfupm.edu.sa
3 School of Civil and Environmental Engineering (SCEE), National University of Sciences & Technology (NUST), Islamabad 44000, Pakistan; imran.nice@nust.edu.pk
4 Department of Chemical Engineering, College of Engineering, King Faisal University (KFU), P.O. Box 380, Al-Hofuf, Al-Ahsa 31982, Saudi Arabia; malfaiad@kfu.edu.sa
* Correspondence: kkhan@kfu.edu.sa (K.K.); mgadir@kfu.edu.sa (M.N.A.); Tel.: +966-13-589-5408 (K.K.); Fax: +966-13-581-7068 (K.K.)

Abstract: The aim of this study was to investigate the influence of fineness and heat-treatment on the pozzolanic and engineering properties of volcanic ash. To this end, two different fineness levels of volcanic ash, ultra-fine (VAF) and fine (VA), without and after heat treatment at different temperatures (VA550, VA650, and VA750), were partially substituted for cement. In addition to the control (100% cement), five binary mortar mixes, each containing 20% of the different types of volcanic ash (VAF and VA; heat-treated and not), were prepared. First, X-ray fluorescence (XRF), X-ray powder diffraction (XRD), particle size analysis, and modified Chappelle tests were used to characterize the material. All mortar mixes were then tested for compressive strength development, water absorption, and apparent porosity. Finally, the microstructure of each of the mixes was evaluated by performing XRD, thermogravimetric analysis (TGA), and Fourier transform infrared spectroscopy (FTIR) analyses on paste samples at 91 days post-formation. The XRD and Chappelle reactivity results revealed increased pozzolanic reactivity with increasing volcanic ash fineness. In contrast, heat treatment adversely affected the pozzolanic reactivity of the volcanic ash due to the formation of crystalline phases at high temperatures. The mortars containing VAF20 (VAF, no heat, at 20%) showed slightly improved compressive strength (69.6 MPa) than the control (68.1 MPa) and all other binary mixes (66.7, 63.5, 64.2, and 63.9 MPa for VA20, VA20-550, VA20-650, and VA20-750, respectively) at 91 days. The mortar containing VAF20 demonstrated the lowest level of water absorption (9.3%) and apparent porosity (19.1%) of all mixes, including the control. The XRD results for the paste samples show that both VA and VAF showed the least intensity of portlandite phase, as compared to the control and other binary mixes. TGA results also show that binary mixes of VA and VAF have a reduced amount of portlandite, resulting in the densification of the mixes' microstructures. With the addition of VAF, there is a significant shift in the FTIR band from 980 to 992 cm^{-1}, which causes the formation of additional C–S–H gels that lead to the densification of the paste matrix. These results demonstrate that VAF exhibits high pozzolanic reactivity, making it suitable for use as a natural pozzolan that can partially substitute cement in the production of strong, durable, and environmentally friendly concrete.

Keywords: volcanic ash; heat treatment; mortar; compressive strength; X-ray powder diffraction; thermogravimetric analysis; Fourier transform infrared spectroscopy analysis

check for updates

Citation: Khan, K.; Amin, M.N.; Usman, M.; Imran, M.; Al-Faiad, M.A.; Shalabi, F.I. Effect of Fineness and Heat Treatment on the Pozzolanic Activity of Natural Volcanic Ash for Its Utilization as Supplementary Cementitious Materials. *Crystals* **2022**, *12*, 302. https://doi.org/10.3390/cryst12020302

Academic Editors: Faheem Ahmed, Nishat Arshi, Shalendra Kumar and Nagih Shaalan

Received: 3 February 2022
Accepted: 18 February 2022
Published: 21 February 2022

Publisher's Note: MDPI stays neutral with regard to jurisdictional claims in published maps and institutional affiliations.

Copyright: © 2022 by the authors. Licensee MDPI, Basel, Switzerland. This article is an open access article distributed under the terms and conditions of the Creative Commons Attribution (CC BY) license (https://creativecommons.org/licenses/by/4.0/).

1. Introduction

A significant amount of natural resources is consumed by buildings and infrastructure, creating an ongoing sustainability challenge. Concrete is the second most consumed material on the planet, after water. In 2006, it was estimated that about 25 billion tons of concrete are produced annually worldwide [1–5]. The production of cement peaked in 2016 at 4 billion tons, which indicates the huge amount of greenhouse gases being released into the atmosphere along with the enormous amount of water and aggregates that are utilized in making concrete. Global cement production accounts for around 7% of total carbon dioxide emissions. In order to produce 1000 kg of cement, 4–7 GJ of energy is required, which releases 800–1000 kg of carbon dioxide gas into the atmosphere. CO_2 emissions contribute to climate change and global warming [6–11]. The demand for low-carbon concrete for climate change mitigation and adaptation increases daily.

In order to reduce the high energy demands and the increased carbon footprint, researchers have suggested multiple techniques, such as carbon capturing and utilization, clinker reduction, alternate fuel sources and modifications in cement manufacturing, etc. [12–14]. It is most effective to replace clinker, the major source of CO_2 emissions in cement production, with alternate materials that have pozzolanic properties or cementitious properties. A wide range of pozzolans and auxiliary cementitious materials (SCM), including fly ash, silica fume, electric arc furnace slag, rice husk ash, wheat straw ash and natural pozzolans [15–22], etc., are used for cement substitution, which helps reduce clinker production and emission of CO_2. The impact of SCMs on the future cement industry will be determined by many factors, including the availability of SCMs, their production efficiency, and cost-effectiveness. Fly ash and slag production is currently estimated at 500 and 300 million tons, respectively [23]. Due to limited supplies, it is usually not possible to reduce CO_2 emissions further with SCMs, such as ground granulated blast furnace slag or fly ash from coal incineration [24] Therefore, there is an urgent need to investigate new cement substitutes to reduce the CO_2 emissions produced by the concrete industry. Naturally occurring pozzolanic materials, such as volcanic ash, volcanic pumice, and calcined clay, which are available in mass amounts, can be used as an alternative to meet the needs of the concrete industry.

Construction in the Kingdom of Saudi Arabia (KSA) has gained pace during the last two decades. KSA has one of the world's highest per capita cement consumption rates, with production estimated at 42.2 million tons in 2019 [25]. In order to meet the local concrete industry's needs, KSA imports a huge amount of SCMs, such as FA, GGBFS, and SF. Recently, natural volcanic pozzolans found in Western KSA, have been identified as a promising partial cement replacement material. A large portion of the basaltic flows in the west of KSA formed millions of years ago. These areas are known as Harrat [26]. The western part of Saudi Arabia is home to several big and small Harrats, spread out over a vast area of km^2 [27]. Both Harrat Rahat and Kishb contain 644 and 163 scoria cones, respectively [28,29]. A total of 327 scoria cones have been found in Harrat Khaybar, Ithnayn, and Kura [30–32]. Scoria has lightweight particles of between 2 and 32 mm in size, with a reddish or black appearance. Scientists have extensively studied the pozzolanic properties of such deposits, finding that the vast majority of samples show pozzolanic activity. The researchers concluded that scoria samples could possibly be used as cement substitutes in concrete [33,34]. Volcanic ash from locally available natural sources can be used as a partial substitute for Portland cement in the production of strong and durable concrete.

Several studies have been performed to investigate the role of natural volcanic ash on the mechanical and microstructural properties of mortar and concrete [35–41] Researchers have documented the significant technical benefits of partially substituting OPC with NP, but they also noted that the early age strength (7 and 28 days) of concrete mixtures using volcanic ash as a substitute for different percentages of cement in the cement mixtures, was lower than that of control samples. In accordance with Moufti et al. [35], finely pulverized scoria passed through a 45 mm sieve with a 10% mass content has a compressive strength comparable to control samples. Sabtan et al. [36] concluded that all samples from the

Harrat region demonstrate pozzolanic behavior and meet Italian requirements. A study by Khan et al. [37] reported that when 15% of natural pozzolans were substituted by cement, the finely ground pozzolans had a lower compressive strength at all ages, as compared to controls. According to Patil et al. [40], volcanic ash substitutions of up to 30% of the mass of OPC led to increased vascularity and porosity of the cementitious matrix. Fadala et al. [42] reported that a 10% substitution of volcanic ash in cement resulted in a minor reduction in strength compared to control samples. Meanwhile, 20% and 30% substitutions of volcanic ash in cement led to significant reductions in strength, at all ages, as compared to control samples. Research studies have shown that volcanic ash has low reactivity, which contributes to delays in the development of strength and other durability characteristics. Therefore, it is imperative that volcanic ash be improved in order to increase its reactivity and ultimately improve its strength and durability. Previous research studies have demonstrated that natural pozzolans can be improved by utilizing mechanical, chemical, and thermal techniques [43–49].

The aim of this study was to determine the influence of fineness and heat treatment of volcanic ash used as a partial replacement for cement to produce a high-performance sustainable mortar. Initially, the ground volcanic ash was passed through sieves No. 450 and 625 to obtain fine volcanic ash (VA) and ultra-fine volcanic ash (VAF). Then, VA was exposed to different elevated temperatures (550, 650, and 750 °C) in a kiln to examine the impact of heat treatment on the pozzolanic properties of VA. Chemical composition analyses, using XRF analysis, particle size analysis, X-ray diffraction analysis (XRD), and modified Chapelle reactivity was performed on both ground (VA, VAF) and heat-treated volcanic ash (VA550, VA650, and VA750). In the second phase, mortar samples were prepared for a control mix and five binary mixes containing 20% volcanic ash (VA, VAF, VA550, VA650, and VA750) as a replacement for cement as shown in Figure 1. Mechanical properties, such as compressive strength (7, 28, and 91 days), water absorption (WA), and apparent porosity (AP) (91 days) were investigated for all of the mortar mixes. Finally, a microstructural investigation of the mixes using XRD, TGA, and FTIR analyses was conducted on the paste samples.

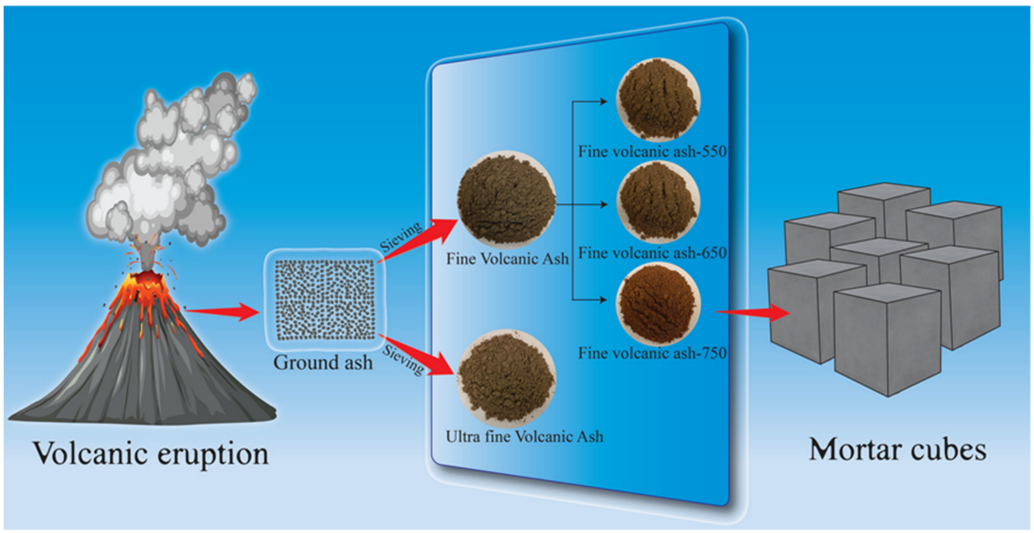


Figure 1. Schematic presentation of the use of volcanic ash for mortar cubes applications.

2. Materials and Methods

2.1. Materials

Ordinary Portland cement I corresponding to ASTM C150 Type I was used as the major binding material [50]. The main binder material had a specific gravity of 3.15 g/cm^3 and a Blaine fineness of 344 m^2/kg. The volcanic ash used in this study was obtained from the western part of the Kingdom of Saudi Arabia. Raw volcanic ash in aggregate form was obtained from a quarry located at Harrat Rahat, Medina province, Saudi Arabia.

The volcanic ash was ground and passed through sieves no. 450 and 625. Sieving was performed to produce VA and VAF to evaluate the effect of fineness on its engineering properties. The volcanic ash passed through sieve no. 450 (VA) was heated at three different temperatures (550, 650, and 750 °C) in order to determine the effect of heat treatment on the mechanical and microstructural properties (Figure 2). An electrical muffle furnace was used to calcine fine volcanic ash (VA) at temperatures of 550 °C, 650 °C, and 750 °C for two hours, and then to allow the ash to air-cool abruptly. The elemental composition of OPC and volcanic ash can be found in Table 1.

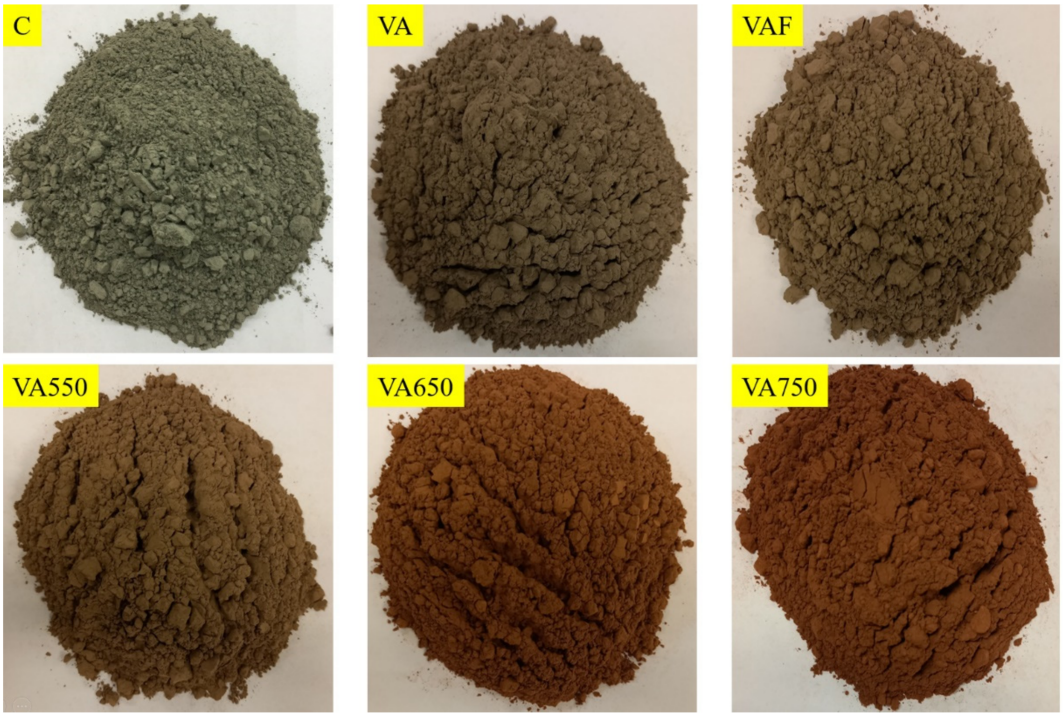


Figure 2. The materials used in this study, in powder form: cement (C); fine volcanic ash (VA); ultra-fine volcanic ash (VAF); and VA at 550 °C (VA550), VA at 650 °C (VA650), and VA at 750 °C (VA750).

Table 1. Physical and chemical composition of cement and volcanic ash.

	C	VA	VAF
	Physical Properties		
Specific gravity (g/cm^3)	3.15	2.64	
Fineness (m^2/kg) (Blain)	344	-	-
Fineness (m^2/cc) (Microtrac S3500)	0.5670	0.816 (<38 μ)	1.194 (<20 μ)
	Chemical properties (oxides, % by weight)		
SiO_2	20.9	46.4	
Al_2O_3	5.18	14.4	
Fe_2O_3	3.04	12.8	
(SiO_2 + Al_2O_3 + Fe_2O_3) *	-	73.6	
CaO	63.9	8.80	
MgO	1.65	8.30	
Na_2O	0.10	3.80	
K_2O	0.52	1.90	
SO_3	2.61	0.80	
LOI **	2.51	2.80	

Table 1. *Cont.*

	C	VA	VAF
		Physical Properties	
		Compounds (%)	
C_2S	52.1	-	
C_3S	19.6	-	
C_3A	8.17	-	
C_4AF	8.81	-	

* ASTM C618-15; ** LOI = loss on ignition.

Figure 3 shows the particle size analysis curves using laser diffraction techniques for C, VA, and VAF. The particle size analysis indicates that both VA and VAF are finer than the control, cement samples. X-ray diffraction analyses (Figure 4) were performed on the raw sample of VA and again once it had been heated to three different temperatures (550, 650, and 750 °C) to investigate how heat treatment impacts the morphology and phases of the samples. Commercially available desert sand was used as a fine aggregate with a fineness modulus of 2.54 and met the standard code provisions esp. EN 196-1: 2016 and ISO 679: 2009 [51,52]. According to ASTM C125, the fineness modulus should be between 2.3 and 3.1 [53].

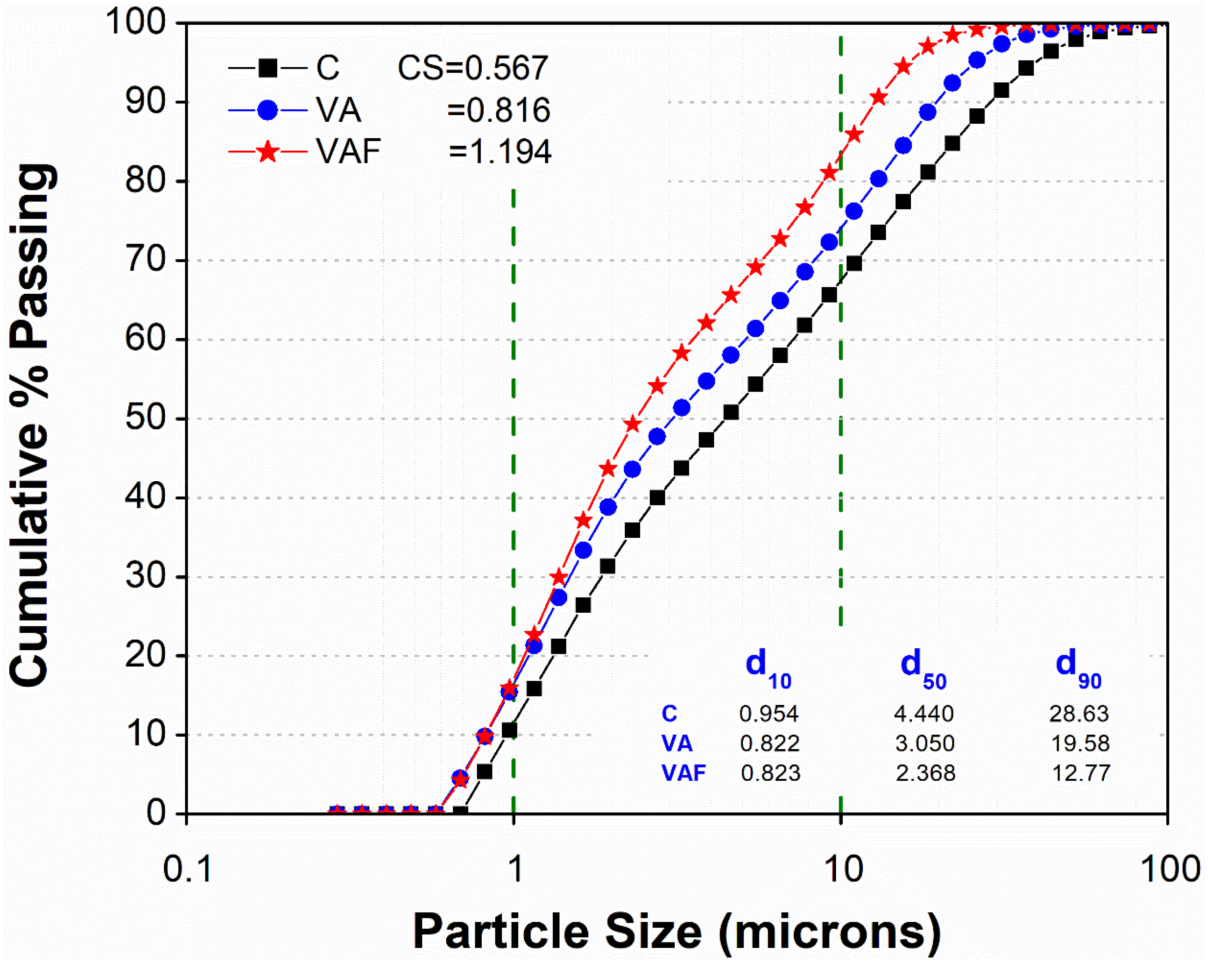


Figure 3. Particle size distribution curves of cement, fine volcanic ash, and ultra-fine volcanic ash.

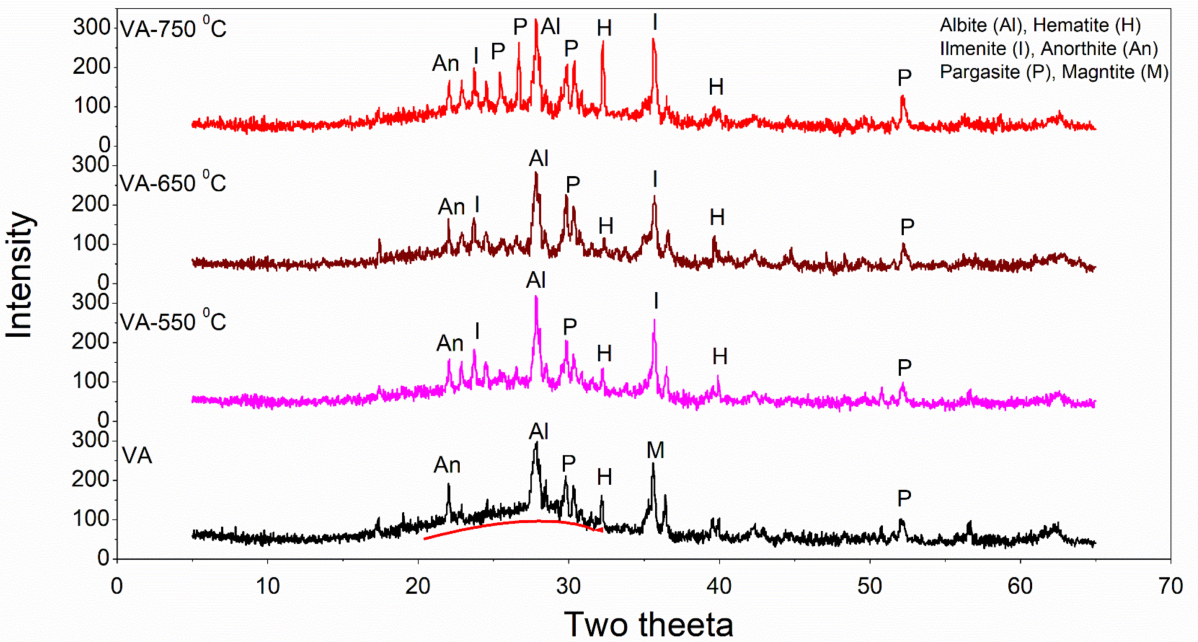


Figure 4. XRD patterns of fine volcanic ash (VA) before and after heat treatment at different temperatures.

2.2. Mix Proportions and Test Methods

2.2.1. Mix Proportions

A total of 72 samples with different mix proportions were cast including the control sample which contained 100% cement as a binder. The different mix proportions in Table 2 show that fine and ultra-fine (VA, VAF) and heat-treated (VA550, VA650, VA750) volcanic ashes were used as a 20% replacement in cement to investigate its effects as a cement substitute in mortar. A 20% substitution of volcanic ash (VA20, VAF20, VA20-550, VA20-650, and VA20-750) along with 80% cement as a binder in terms of quantity, was used in this study. Different mix IDs represent the composition of the constituent binders e.g., VA20 represents 80% of C and 20% of VA, whereas VA20-550 represents 80% of C and 20% of VA exposed to 550 °C, etc. Compressive strength tests were conducted on 50 mm^3 samples after curing for 7, 28, and 91 days. Water absorption capacity and porosity were simultaneously calculated on 50 mm^3 samples after 91 days of curing. For all tests, three samples were tested and an average was taken as the final result. The water to binder ratio in the mortar was maintained in accordance with standard code provisions (ASTM C109) [54].

Table 2. Mixture proportions of mortar (w/cm = 0.40; cm:s = 1:1.36).

Batch Quantities (g) for Nine 50-mm^3 Mortar Specimens					
Mix ID	**Water (w)**	**Cement (c)**	**VA**	**VAF**	**Sand (s)**
Control Mortar (CM)	440	1100	0	0	1500
20% VA (VA20)	440	880	220	0	1500
20% VAF (VAF20)	440	880	0	220	1500
20% VA550 (VA20-550)	440	880	220	0	1500
20% VA650 (VA20-650)	440	880	220	0	1500
20% VA750 (VA20-750)	440	880	220	0	1500

2.2.2. Mixing and Testing for Compressive Strength of Mortar Cubes

A three-speed Hobart mixer was used to mix the constituents of mortar according to ASTM C305 [55]. Initially, the binder and water were mixed for 30 s at a low speed. The sand was then added while the mixing speed was kept constant. Then, the mixer speed was increased to an intermediate level, and stirring continued for 30 s. The mixing was stopped for 90 s and was then resumed at a medium speed for 60 s in the final stage. Total mixing time for the whole process was 4 min, using the same Hobart mixer for each mixture. A constant flow of between (15–115%) was maintained (ASTM C1467) for all mixes by adding a naphthalene sulphonate-based superplasticizer. Based on the mixer's capacity, mixing was performed in order to cast twelve 50 mm^3 samples for each mix. Immediately after mixing, casting took place. The fresh mortar was filled in two layers into a 50 mm^3 steel mold which had been oiled on the inside. Roding was performed after each layer was filled, in accordance with the ASTM C109 code [54]. To test compressive strength (7, 28, and 91 days) and porosity and water absorption (91 days), 12 samples of each mix were cast (Table 2). After casting, the samples were covered by plastic sheets to prevent any loss of water. Samples were demolded after 24 h and kept in a water tank to cure until the testing age.

The cured mortar cubes were taken from the curing tanks after completing the required curing duration and were subsequently tested for compressive strength. Testing was carried out in accordance with the relevant ASTM C109 codes. A universal testing machine (UTM) was used for testing the mortar samples. The UTM had a capacity of 300 kN and the rate of strain was maintained as 1 mm/min. A data logger was attached to the transducers and strain gauges which recorded all the readings automatically. The peak strength was calculated as the ratio of the maximum load at failure, to the area of the sample (here 2500 mm^2). Water absorption capacity and apparent porosity were calculated as per ASTM C 948-81 [56]. For all testing, the average value of three samples was taken as the final reading.

2.3. Modified Chappelle Test to Evalute the Reactivity of Pozzolanic Materials

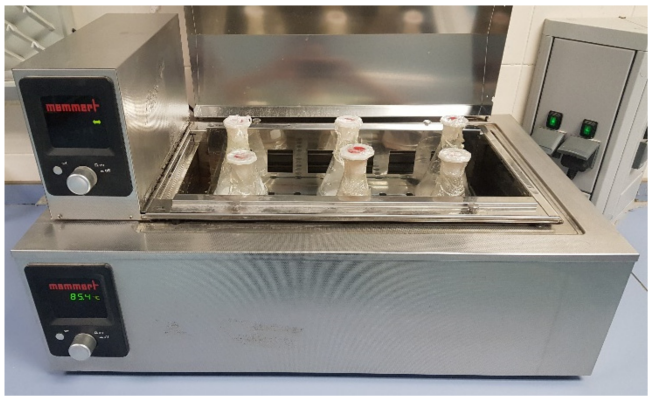
The reactivity of pozzolans can be evaluated chemically by using a Chapelle activity test. The test adhered to the NF P 18-531 standard, as follows Figure 5): 2 g of CaO was mixed with 1 g of pozzolanic material, together with 250 mL of deionized water in an Erlenmeyer flask. The flask was placed in a hot water bath with a shaker at 90 ± 5 °C for 16 ± 2 h. The solution was then cooled to room temperature; 250 mL of sucrose solution (240 g/L) were added to the flasks and mixed for 15 min. The solution was then filtered and 25 mL of the filtrate was tittered with 0.1 M HCl solution using phenolphthalein as indicator. Chapelle activity was calculated by:

$$mg\ CaO\ per\ gram\ of\ material = \frac{(28)(2)(2)F_c(v_3m_3 - v_2)}{m_4m_3m_2} \quad (1)$$

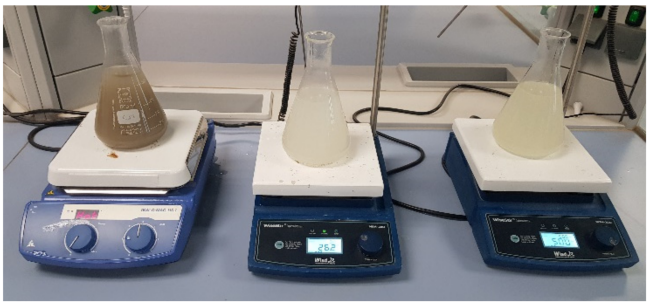
m_2 = grams of pozzolanic material; m_3 = grams of CaO mixed with pozzolanic material; m_4 = grams of CaO in the blank test; v_2 = milliliters of HCl 0.1M consumed by the sample solution; v_3 = milliliters of HCl 0.1 M consumed by the blank solution; F_c = correction factor of HCl 0.1 M standard solution.

2.4. Microstructure Analysis of Pastes Containing Pozzolanic Materials

The microstructural investigation, such as X-ray diffraction analysis, Fourier transform infrared spectroscopy analysis, and thermogravimetric analysis was performed on the cement pastes samples. A detailed description of each technique is discussed below.



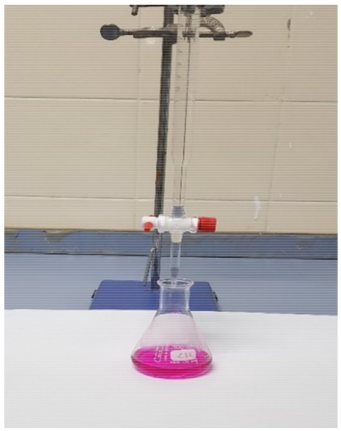
(**a**)



(**b**)



(**c**)



(**d**)

Figure 5. Illustration of the several steps performed to determine Chappelle activity. (**a**) Samples and blank placed in the water bath; (**b**) mixing after adding sucrose solution; (**c**) filtration of the samples; and (**d**) The filtrated sample.

2.4.1. X-ray Diffraction (XRD) Analysis

The crystal structure of the samples was determined via Rigaku CuKα radiation using a bench top Mini Flex X-ray diffraction (mini-XRD) instrument. The patterns were measured from 2θ = 5 up to 80° with a step size and scan speed of 0.02 and 2° per minute, separately. XRD analysis was performed to determine the distinct phases prevalent in the VA paste and to obtain an indication of the reactivity potential of the mixture. This technique was required to understand the crystalline or pozzolanic behavior of the materials.

2.4.2. Thermogravimetric Analysis (TGA)

In addition, thermogravimetric analysis (TGA) was performed on the samples using a Mettler Toledo instrument at a temperature ranging from 25 to 800 °C with a heating rate of 10 °C min^{-1}. All thermogravimetric experiments were conducted under air. Through TGA, the distinct phases in cement paste were determined and the extent of pozzolanic reaction was measured by measuring the consumption of the CH phase.

2.4.3. Fourier Transform Infrared Spectroscopy (FTIR) Analysis

FTIR (Fourier transform infrared spectroscopy, Nicolet NEXUS-FTIR-670 spectrometer) was used to identify vibrations. FTIR was performed using a sample (0.22 vol%) and KBr (50 mg) mixed into a wafer and placed into a self-made cell. A spectrum was then recorded. Cement paste samples were analyzed with FTIR in order to determine any changes in the spectra which indicated that the mineralogical arrangement had changed.

3. Results and Discussions

3.1. Material Characterisations by XRF and XRD Analysis

Table 1 shows the chemical composition of raw volcanic ash determined by XRF analysis. Silica (SiO_2), Alumina (Al_2O_3), Iron oxide (Fe_2O_3), Calcium oxide (CaO), and Magnesia (MgO) are the major elements present in VA. In terms of weight content, silica has the highest value (47.02 wt.%). The sum of SiO_2, Al_2O_3, and Fe_2O_3 is around 70%, which shows that VA fulfills the minimum requirements set by ASTM C618-15 [57] for natural pozzolans.

The XRD analysis of the raw volcanic ash (VA, VAF) and the heat-treated volcanic ash (VA550, VA650, and VA750) are shown in Figure 4. An XRD pattern of the raw volcanic ash showed significant amounts of amorphous glass. Figure 4 shows a broad pozzolanic hump of around 21° to 38° with few distinct crystalline peaks. The peaks in the volcanic ash sample became sharper and more intense when heated at different temperatures. Moreover, new crystal phases evolved, such as hematite, ilmenite, parasite, etc., which changed the color of VA from black to deep red. Many factors could have contributed to this transformation, including the recrystallization of minerals, oxidation of iron oxides, and a transformation into hematite. By increasing the heating temperature, the peaks on the XRD scale became sharper, indicating a further crystallization of hematite and other minerals phases, which ultimately led to a decrease in the amorphous phases.

FTIR analysis (Figure 6) shows the infrared spectrum of the raw volcanic ash (VA, VAF) and the heat-treated volcanic ash (VA550, VA650, and VA750). It is believed that the bands located between 920 and 990 cm^{-1} are caused by the stretching of the Si–O–Al bonds. Quartz minerals possess a vibration mode of Si–O at 558 cm^{-1}. Water molecules vibrate in the O–H mode around 3324 cm^{-1} [58,59]. The IR bands show that the relative intensity of the Si–O–Si band is higher in the raw volcanic ash (VA) as compared to the heat-treated volcanic ashes. The results further demonstrate that Si–O–Si for VA is more broad and wide as compared to the heat-treated sample, which shows the availability of a high amount of amorphous silica present in the sample. The results of this FTIR analysis are consistent with the XRD analysis.

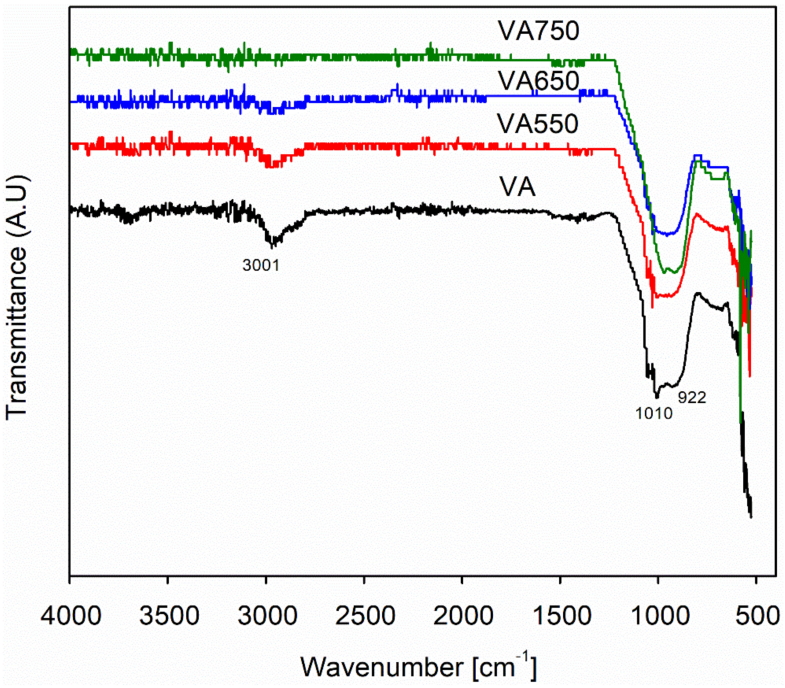


Figure 6. FTIR intensities for untreated VA and heat-treated VA at 550, 650, and 750 °C.

3.2. Chappelle Reactivity Test

Chapelle reactivity is used to measure the amount of CaO consumed by pozzolans; a greater value of Chapelle reactivity indicates better pozzolanic reactivity of a given sample. According to the test results presented in Table 3, the VAF sample demonstrated the highest level of reactivity among the samples. These results indicate that the particle size of the material can greatly affect its reactivity with CaO. In addition, both VA and VAF exhibited better pozzolanic reactivity compared to the heat-treated VA (VA550, VA650, and VA750). Furthermore, VA samples exposed to high temperatures (VA650 and VA750) showed the lowest Chapelle reactivity values. The reduction in pozzolanic reactivity can be attributed to the formation of crystalline phases at high temperatures. The Chappelle test results are also in agreement with those from the XRD analysis and the other tests conducted in this study.

Table 3. Chappelle test results of VA, VAF, and heat-treated VA550, VA650, and VA750 according to NF P 18-531.

Materials	Chappelle Activity (mg CaO/g Sample)
VA	821.51
VAF	844.32
VA550	808.75
VA650	792.80
VA750	800.29

3.3. Influence of Fineness and Heat-Treatment on Strength, Porosity, and Water Absorption

Figure 7 shows a comparison of the compressive strength test results of the control mortar (CM) and the binary mortar containing 20% VAF, both before (VA20) and after heat treatment at 550 °C (VA20-550), 650 °C (VA20-650), and 750 °C (VA20-750). As compared to the control, the compressive strength of VA20 decreased at all ages. However, the intensity of the strength reduction was significantly reduced at later ages, where a comparable 91-day strength was observed to that of CM. Moreover, due to increasing fineness, a slight increase in strength was observed for VAF20 as compared to VA20. However, despite increased fineness, the compressive strength of VAF20 remained lower than that of CM at all ages, except at 91 days, where a slightly higher strength, as compared to CM, was observed. An improved later age strength for both VA20 and VAF20 is attributed to the delayed pozzolanic action of VA. Similar results were reported by other researchers where the strength of mortar at early ages (7 or 28 days) was reduced due to adding 20% fly ash or 20% waste glass sludge as a replacement of cement [34,60]. However, at later ages (91 days), similar to the findings of the current study, a comparable strength to that of the control mortar was observed in these studies. Unlike the positive influence of increased fineness, the negative impact of heat treatment on strength was observed in all mortar mixes (VA20-550, VA20-650, VA20-750), especially at later ages. For instance, the compressive strength of mortar mixes containing heat-treated VA, slightly decreased as compared to untreated VA at all ages (28 and 91 days), except at early ages (7 days). This decrease in the strength of mortar containing the heat-treated VA is due to the transformation of the nature of VA from amorphous to crystalline. However, at early ages, a slight rise in strength occurs due to an improvement in the cementitious potential of VA following heat treatment. The closeness of the strength test results, irrespective of aging, among all mortars containing treated VA, demonstrates an insignificant effect of increasing heat treatment temperatures. Therefore, the current results suggest that mechanical treatment of VA alone should be used to obtain an optimized fineness and the best strength potential and that heat treatment should not be used, to avoid compromising strength potentials.

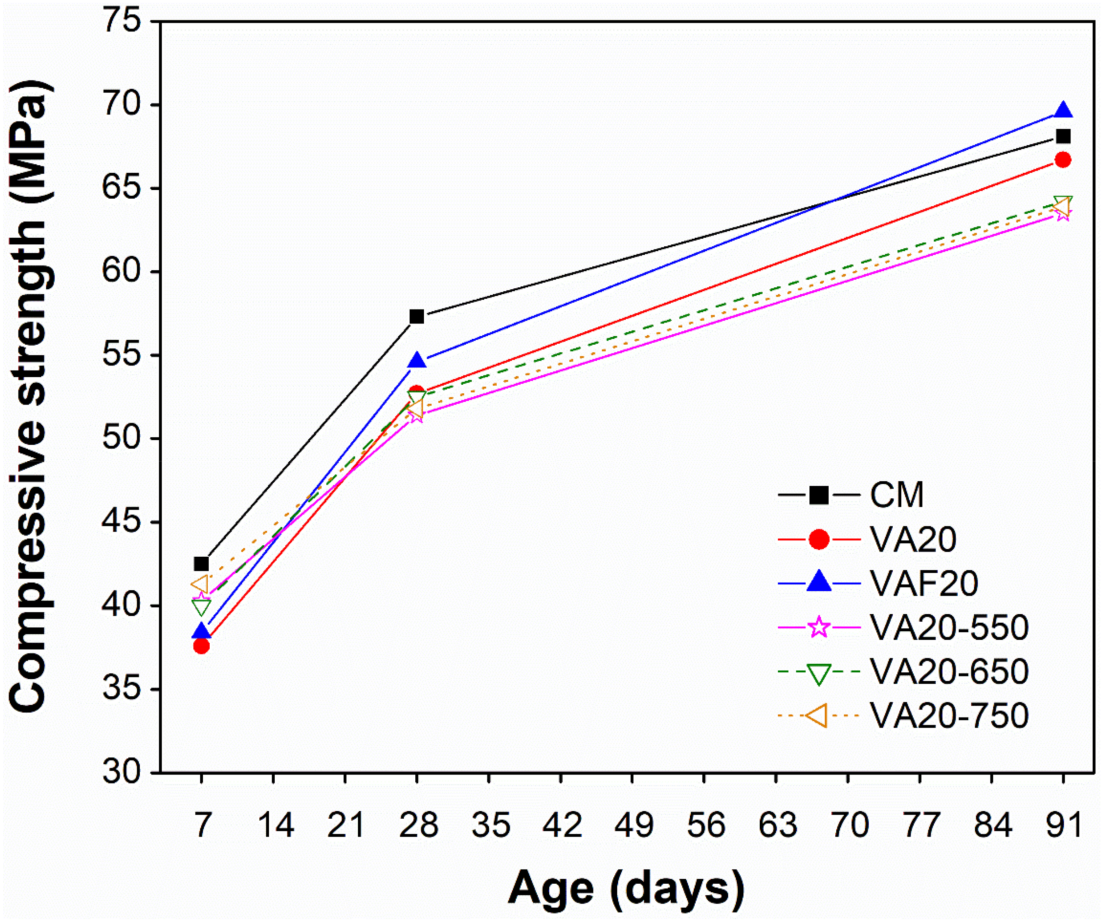


Figure 7. Comparison of compressive strength development between control and mortar containing VAF, and heat-treated and untreated VA.

Like compressive strength, very similar trends of water absorption and apparent porosity were observed among all mortars (Figure 8), which indirectly validates the strength results. For instance, a slight increase in WA and AP values was observed for VA20 as compared to CM, while VAF20 exhibited lower values as compared to both CM and VA20 due to its decreased particle sizes, which ultimately would lead to better packing and filling abilities along with improved pozzolanic action. Once again, a negative impact of heat treatment was also observed for WA and AP among mortars containing heat-treated VA. The results show that WA and AP values for mortars containing heated-treated VA were higher as compared to mortar containing untreated VA or CM. This ultimately validates the lower strength results of mortar having treated VA.

3.4. X-ray Diffraction of Cement Pastes Containing Pozzolanic Materials

Figure 9 shows the XRD analysis peak results for paste samples of control and binary mixes containing 20% volcanic ashes (VA, VAF, VA550, VA650, and VA750) as a replacement for cement. Pozzolans contain amorphous and glassy silica which forms calcium silicate hydrate (CSH) when it reacts with portlandite ($Ca(OH)_2$). During the pozzolanic reaction, the pozzolans combine with the portlandite phase in the cement matrix and produce additional C–S–H gels, which mainly contribute toward strength development. Therefore, the depletion of the portlandite phase in cement paste can be used to determine the pozzolanic potential of cement substitutes [61,62]. A comparison of the XRD patterns of the cement pastes from the mixes was conducted for their peak $Ca(OH)_2$ intensity, which corresponded to 18.02° two-theta at 91 days, as shown in Figure 9.

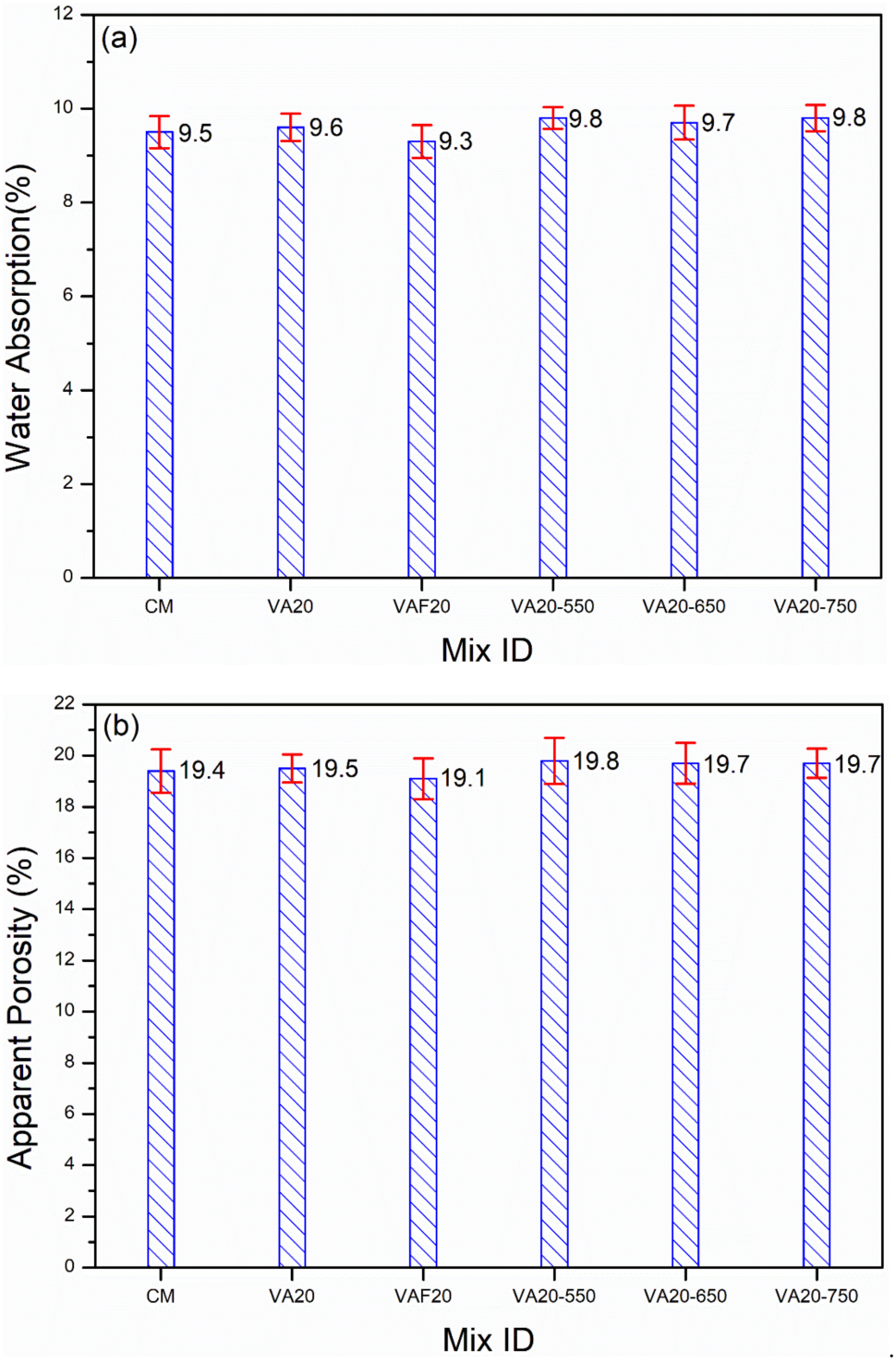


Figure 8. Comparison of (**a**) water absorption, (**b**) apparent porosity results between control, and mortar containing VAF, and heat-treated and untreated VA after 91 days of standard curing.

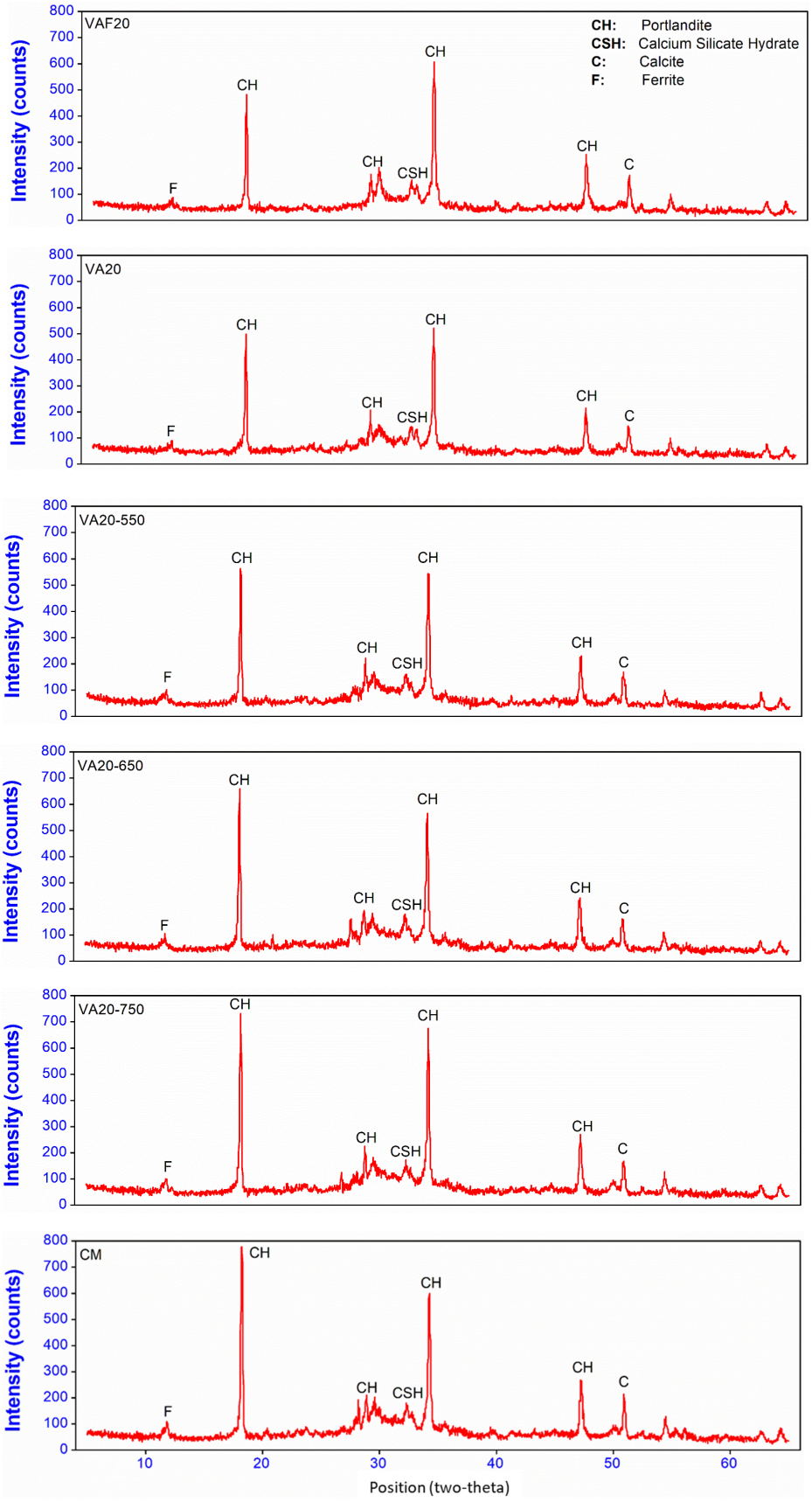


Figure 9. Comparison of XRD peaks between the control mortar (CM) paste and pastes containing different volcanic ashes at 91 days.

The intensity of $Ca(OH)_2$ for the control sample is the highest among all other samples. The high amount of cement present in the control samples led to hydration, resulting in the formation of a significant amount of $Ca(OH)_2$ in the samples. The XRD results also demonstrate that the VAF samples showed the least amount of the portlandite phase as compared to all other samples. This indicates that VAF possesses better pozzolanic reactivity, due to the presence of amorphous silica, which consumes the portlandite phases to form additional CSH phases. However, the cement paste samples containing heat-treated volcanic ash (VA550, VA650, and VA750) had a high intensity of $Ca(OH)_2$, which is indicative of low reactivity due to the formation of a crystalline phase at high temperatures. Among all blended samples, the VA750 sample showed the highest level of $Ca(OH)_2$, indicating the presence of a large number of crystalline phase.

3.5. Thermo Gravimetric Analysis (TGA) of Cement Pastes Containing Pozzolanic Materials

Thermogravimetric analysis was used to measure the amount of $Ca(OH)_2$ in the cement paste samples due to the weight loss that occurred between 400 °C and 500 °C after thermal decomposition [63,64]. The thermogravimetric analysis was performed on the paste samples, including control mixes (C) and the binary mixes (VA, VAF, VA550, VA650, and VA750) at 91 days age, as shown in the Figure 10.

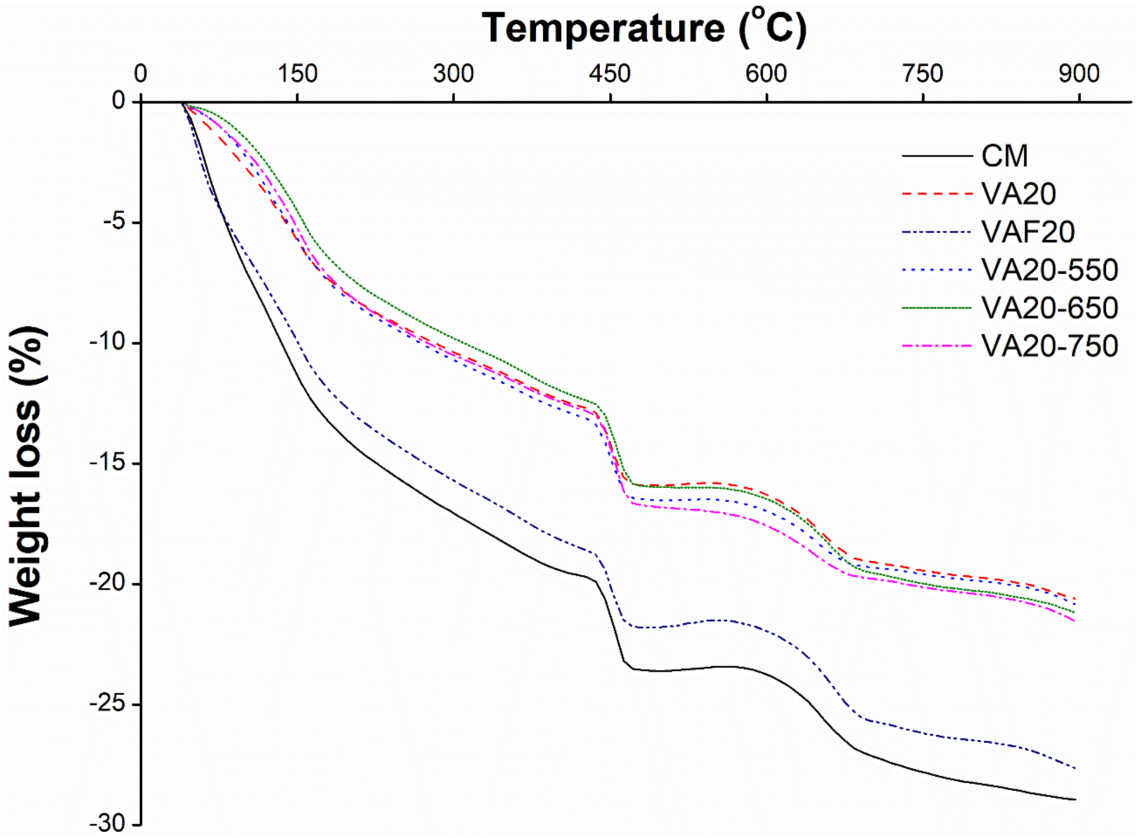


Figure 10. TGA results for control mortar (CM) paste and pastes containing different volcanic ashes at 91 days.

The TGA results shows that the control mix (CM) demonstrated the greatest amount of portlandite (C–H), when compared to the other mixes. The binary mix with 20% VAF, recorded the least amount of portlandite phase among the mixes. This significant reduction is attributed to the high reactivity of the very fine amorphous silica in the VAF sample, causing greater consumption of the C–H phase to form additional C–S–H phases in the paste matrix. Further, the VA sample also exhibits a better reduction of the portlandite (C–H) phase, which is attributed to an amorphous silica present in the VA sample. However, the

heat-treated samples (VA550, VA650, and VA750) exhibited a lower reduction of portlandite, indicating low reactivity of these materials due to the development of a crystalline phase at high temperatures.

3.6. Fourier Transform Infrared Spectroscopy (FTIR) Analysis of Cement Pastes Containing Pozzolanic Materials

IR bands are visible at the same location in all paste samples, but at varying intensities, as shown in Figure 11. This is primarily attributed to the formation of the C–S–H and C–H phases. Si–O bonds in the C–S–H phase are responsible for the peaks between 900 cm^{-1} and 1100 cm^{-1} [65]. The IR bands show that the relative intensity of the Si–O band is higher in VAF as compared to the other binary mixes and the control sample. The Si–O band in the VAF samples is broad and shifts toward a high wavelength (992 cm^{-1}), which indicates high silica polymerization, which is ultimately responsible for the maximum number of high-density C–S–H phases. The formation of high-density C–S–H phases causes densification of the micro and pore structure, resulting in better mechanical performance. In addition, the VA sample showed a slight increase in the intensity of Si–O bands (984 cm^{-1}) as compared to the control sample, which is an indication of the low pozzolanic reactivity of VA as compared to VAF. The heat-treated volcanic ashes (VA550, VA650, and VA750) showed a decrease in the intensity of the Si–O band, which indicates poor pozzolanic reactivity, which leads to the formation of low density C–S–H phases and ultimately affect its engineering performance.

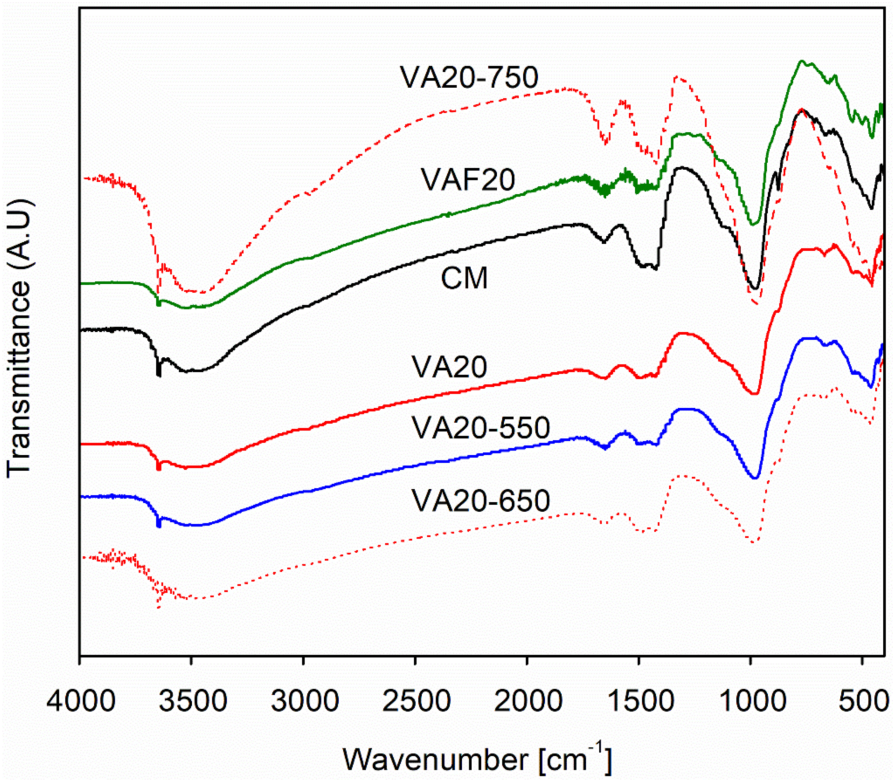


Figure 11. FTIR intensities for control mortar (CM) paste and pastes containing different volcanic ashes at 91 days.

In all the samples tested, the peak at 3645 cm^{-1} shows the presence of free OH groups, indicating the existence of the portlandite phase [66]. The peak at 3645 cm^{-1} is wide and more visible in the control sample. For the binary mixes, this peak became smaller which indicates pozzolanic reactivity of the volcanic ashes by utilizing $Ca(OH)_2$. The portlandite peak is very small for VA, and is especially so in the VAF sample, as compared to the other blended samples, which show better reactivity of fine and ultra-fine volcanic ash,

which ultimately lead to the formation of a more refined microstructure, resulting in better mechanical performance.

4. Conclusions

The purpose of the current study was to evaluate the impact of fineness and heat treatment on the performance of natural volcanic ash, used as a cement substitute to produce a sustainable and high-performance mortar. Along with the control (100% cement), five binary mixes of volcanic ash (VA, VAF, VA550, VA650, and VA750) were selected. The effect of fineness and heat-treatment on the mechanical properties (compressive strengths, WA, and AP) was examined. Furthermore, XRD, FTIR, and TGA analyses were conducted to investigate the effect of volcanic ash on the microstructure of the cemented paste.

The results of this study led to the following conclusions:

- The X-ray diffraction and Chapelle reactivity results indicate that pozzolanic reactivity increases with fineness. Therefore, ultra-fine volcanic ash (VAF) showed highest value of Chapelle reactivity due to the availability of very fine amorphous silica. Heat-treated volcanic ashes (VA-550, VA-650 and VA-750), on the other hand, had comparatively reduced pozzolanic reactivity due to the crystallization of the existing phases and the formation of new crystalline phases, when exposed to high temperatures.
- An improvement in compressive strength was observed in a mortar containing 20% VAF (69.6 MPa) due to increasing the fineness of VA, as compared to CM (68.1 MPa), especially at 91 days. The above results were validated by VAF20 being shown to have the lowest WA (9.3%) and AP (19.1%) capacity at 91 days among all mixes. Moreover, the negative impact of heat treatment on VA (at 550, 650, and 750 °C) was observed in terms of strength. The strength of the mortar containing heat-treated VA was slightly reduced (63.5, 64.2 and 63.9 MPa for VA20-550, VA20-650, and VA20-750, respectively) as compared to the control (68.1 MPa) or untreated VA (66.7 MPa). This is attributed to the change of the amorphous nature of the VA into crystalline, due to the heat treatment. The current findings suggest that grinding VA to increase its fineness is the most effective and viable approach to achieving optimal engineering performance.
- X-ray diffraction analysis results on the paste samples showed that the binary mixes with 20% VAF (VAF20) significantly reduced the intensity of calcium hydroxide due to its better pozzolanic behavior as compared to the other mixes. This resulted in the better pozzolanic reactivity of VAF in the paste matrix. The mixes having heat-treated volcanic ashes (VA20-550, VA20-650, and VA20-750) showed high intensities of portlandite peaks, which indicates that these volcanic ashes have low reactivity; therefore, they do not significantly contribute to the improvement of micro and pore structure. TGA analysis also showed that the portlandite phase is significantly reduced in binary mixes containing fine and ultra-fine volcanic ashes (VA20 and VAF20), as compared to the other mixes (including the control mix). This indicates the superior pozzolanic property of the fine amorphous silica present in these samples. On the other hand, heat-treated samples (VA20-550, VA20-650, and VA20-750) showed a high amount of portlandite phase among all binary mixes, due to its low reactivity, as was also shown by the XRD results and the results of the Chappelle reactivity test.
- FTIR analysis results showed a shift in the Si–O–Si band with the addition of fine and heat-treated volcanic ashes in the binary mixes. This shift (980 to 992 $cm^{-1)}$ was more pronounced in the binary mix containing VAF, which indicates the presence of a large number of high-density C–S–H phases, causing densification of the micro and pore structure of the paste mix. In addition, the portlandite peaks (3640 cm^{-1}) are significantly reduced in VA20 and VAF20 mixes, as compared to other binary mixes, which shows the superior reactivity of fine VA, that ultimately results in the formation of more C–S–H phases, causing densification of paste matrix.

Author Contributions: K.K. and M.N.A. contributed to the design of this research project. K.K., M.N.A. and M.U. contributed to performing the experiments starting with the collection of all

materials, sieving VA to obtain desired fineness, mixing, casting, demolding, curing of mortar cubes. K.K. performed the compressive strength tests on mortar cubes and measured water absorption and porosity at different ages. M.A.A.-F. performed the Chapple reactivity test. M.I. and M.U. supported in the particle size analysis and the XRD, TGA, FTIR analyses of materials and pastes. All authors (K.K., M.N.A., M.U., M.I., M.A.A.-F. and F.I.S.) contributed to the preparation of the initial draft of this manuscript. K.K. and M.N.A. critically analyzed and discussed the results of this research and prepared the final draft of this manuscript. At the revision stage, K.K. and M.N.A. contributed to the revision and prepared the final revised manuscript. All authors have read and agreed to the published version of the manuscript.

Funding: The Deanship of Scientific Research (DSR) at King Faisal University (KFU) financially supported this research through its Nasher Track "Grant Number 216010".

Institutional Review Board Statement: Not applicable.

Informed Consent Statement: Not applicable.

Data Availability Statement: All the data utilized in current research are available on a reasonable request from the corresponding author.

Acknowledgments: This research was supported by the Deanship of Scientific Research (DSR) at King Faisal University (KFU), through Nasher Track Grant Number 216010. The authors wish to express their gratitude for the financial support that made this study possible. The authors also extend their appreciation to Department of Civil Engineering at King Faisal University, Saudia Arabia for providing its lab facilities to conduct the required experimental tasks.

Conflicts of Interest: The authors declare no conflict of interest. The founding sponsors had no role in the design of the study; in the collection, analyses, or interpretation of data; in the writing of the manuscript, or in the decision to publish the results.

References

1. Yang, K.H.; Jung, Y.B.; Cho, M.S.; Tae, S.H. Effect of supplementary cementitious materials on reduction of CO_2 emissions from Concrete. In *Handbook of Low Carbon Concrete*, 1st ed.; Butterworth-Heinemann: Oxford, UK, 2017; pp. 89–110.
2. Klee, H. *The Cement Sustainability Initiative: Recycling Concrete-Summary*; World Business Council for Sustainable Development (WBCSD): Geneva, Switzerland, 2009.
3. Abergel, T.; Dean, B.; Dulac, J. Global status report 2017: Towards a zero-emission, efficient, and resilient buildings and construction sector. *U. N. Environ. Program.* **2017**, *48*, 1–48.
4. IEA-WBCSD, Cement Technology Roadmap 2009—Carbon Emissions Reductions up to 2050. Available online: https://www.iea.org/publications/freepublications/publication/Cement.pdf (accessed on 25 January 2022).
5. Coffetti, D.; Crotti, E.; Gazzaniga, G.; Carrara, M.; Pastore, T.; Coppola, L. Pathways towards sustainable concrete. *Cem. Concr. Res.* **2022**, *154*, 106718. [CrossRef]
6. Emmanuel, H.; Marine, S.; Gondia, S.S.; Clément, B.; Aymen, J.; Samuel, C. The impact of future power generation on cement demand: An international and regional assessment based on climate scenarios. *Int. Econ.* **2020**, *163*, 114–133.
7. Ozbay, E.; Erdemir, M.; Durmuş, H.I. Utilization and efficiency of ground granulated blast furnace slag on concrete properties—A review. *Constr. Build. Mater.* **2016**, *105*, 423–434. [CrossRef]
8. Abolhasani, A.; Samali, B.; Dehestani, M.; Libre, N.A. Effect of rice husk ash on mechanical properties, fracture energy, brittleness and aging of calcium aluminate cement concrete. *Structures* **2021**, *36*, 140–152. [CrossRef]
9. Qudoos, A.; Kim, H.G.; Atta-ur-Rehman; Jeon, I.K.; Ryou, J.-S. Influence of the particle size of wheat straw ash on the microstructure of the interfacial transition zone. *Powder Technol.* **2019**, *352*, 453–461. [CrossRef]
10. Rahla, K.M.; Mateus, R.; Bragança, L. Comparative sustainability assessment of binary blended concretes using Supplementary Cementitious Materials (SCMs) and Ordinary Portland Cement (OPC). *J. Clean. Prod.* **2019**, *220*, 445–459. [CrossRef]
11. Amin, M.N.; Khan, K.; Saleem, M.U.; Khurram, N.; Niazi, M.U.K. Aging and Curing Temperature Effects on Compressive Strength of Mortar Containing Lime Stone Quarry Dust and Industrial Granite Sludge. *Materials* **2017**, *10*, 642. [CrossRef] [PubMed]
12. Habert, G.; Miller, S.A.; John, V.M.; Provis, J.L.; Favier, A.; Horvath, A.; Scrivener, K.L. Environmental impacts and decarbonization strategies in the cement and concrete industries. *Nat. Rev. Earth Environ.* **2020**, *1*, 559–573. [CrossRef]
13. Garba, M.D.; Usman, M.; Khan, S.; Shehzad, F.; Galadima, A.; Ehsan, M.F.; Ghanem, A.S.; Humayun, M. CO_2 towards fuels: A review of catalytic conversion of carbon dioxide to hydrocarbons. *J. Environ. Chem. Eng.* **2021**, *9*, 104756. [CrossRef]
14. Muhammad, U.; Naseem, I.; Tayyaba, N.; Neelam, Z.; Aisha, A.; Mahmoud, M.A.; Ahmad, G.; Aasif, H. Advanced strategies in Metal-Organic Frameworks for CO_2 Capture and Separation. *Chem. Rec.* **2021**. [CrossRef]
15. Khotbehsara, M.M.; Mohseni, E.; Yazdi, M.A.; Sarker, P.; Ranjbar, M.M. Effect of nano-CuO and fly ash on the properties of self-compacting mortar. *Constr. Build. Mater.* **2015**, *94*, 758–766. [CrossRef]

16. Mazloom, M.; Ramezanianpour, A.A.; Brooks, J.J. Effect of silica fume on mechanical properties of high-strength concrete. *Cem. Concr. Compos.* **2004**, *26*, 347–357. [CrossRef]
17. Amin, M.N.; Khan, K.; Saleem, M.U.; Khurram, N.; Niazi, M.U.K. Influence of mechanically activated electric arc furnace slag on compressive strength of mortars incorporating curing moisture and temperature effects. *Sustainability* **2017**, *9*, 1178. [CrossRef]
18. Khan, K.; Ullah, M.F.; Shahzada, K.; Amin, M.N.; Bibi, T.; Wahab, N.; Aljaafari, A. Effective use of micro-silica extracted from rice husk ash for the production of high-performance and sustainable cement mortar. *Constr. Build. Mater.* **2020**, *258*, 119589. [CrossRef]
19. Amin, M.N.; Murtaza, T.; Shahzada, K.; Khan, K.; Adil, M. Pozzolanic Potential and Mechanical Performance of Wheat Straw Ash Incorporated Sustainable Concrete. *Sustainability* **2019**, *11*, 519. [CrossRef]
20. Játiva, A.; Ruales, E.; Etxeberria, M. Volcanic Ash as a Sustainable Binder Material: An Extensive Review. *Materials* **2021**, *14*, 1302. [CrossRef] [PubMed]
21. Pang, L.; Liu, Z.; Wang, D.; An, M. Review on the Application of Supplementary Cementitious Materials in Self-Compacting Concrete. *Crystals* **2022**, *12*, 180. [CrossRef]
22. Wang, Q.; Ma, Y.; Wang, F.; Shi, Z.; You, H.; Tian, Y.; Liu, Y.; Hu, Z.; Song, H.; Wang, D.; et al. Experimental Study on Carbonation Durability of Kaolin Strengthened with Slag Portland Cement. *Materials* **2022**, *15*, 1240. [CrossRef]
23. Mehta, P.K. Sustainable cements and concrete for the climate change era—A review. In *Proceedings of the Second International Conference on Sustainable Construction Materials and Technologies*; Università Politecnica delle Marche: Ancona, Italy, 2010.
24. Scrivener, K.L.; John, V.M.; Gartner, E.M. Eco-efficient cements: Potential, economically viable solutions for a low-CO_2 cement-based materials industry. *Cem. Concr. Res.* **2016**, *114*, 2–26. [CrossRef]
25. Cembureau. *Activity Report 2020 of The European Cement Association*; Cembureau: Bruxelles, Belgium, 2020.
26. Camp, V.E.; Roobol, M.J. The Arabian continental alkali basalt province: Part 1. Evolution of Harrat Rahat, Kingdom of Saudi Arabia. *Bull. Geol. Soc. Am.* **1989**, *101*, 71–95. [CrossRef]
27. Roobol, M.J.; Pint, J.J.; Al-Shanti, M.A.; Al-Juaid, A.J.; Al-Amoudi, S.A.; Pint, S.; Al-Eisa, A.M.; Allam, F.; Al-Sulaimani, G.S.; Banakhar, A.S. Preliminary Survey for Lavatube Caves on Harrat Kishb. In *Open-File Report SGS-OF-2002-3*; Saudi Geological Survey: Jeddah, Saudi Arabia, 2002.
28. Camp, V.E.; Roobol, M.J.; Hooper, P.R. The Arabian continental alkali basalt province: Part III, Evolution of Harrat Kishb, Kingdom of Saudi Arabia. *Bull. Geol. Soc. Am.* **1992**, *104*, 379–396. [CrossRef]
29. Camp, V.E.; Roobol, M.J.; Hooper, P.R. The Arabian continental alkali basalt province: Part II. Evolution of Harrats Khaybar, Ithnayn and Kura, Kingdom of Saudi Arabia. *Bull. Geol. Soc. Am.* **1991**, *103*, 363–391. [CrossRef]
30. Al-Nakhebi, Z.; Laurent, D. Prospecting for Pozzolan in Midwest Harrat Rahat. In *Open-File Report BRGM-OF-05-15*; Saudi Arabian Deputy Ministry for Mineral Resources: Jeddah, Saudi Arabia, 1985.
31. Sabbahi, A.A. Geology and Resources of Basalt Quarry Site Kishb-12, Southern Harrat Kishb. In *Open File Report SGS-OF-2002-1*; Saudi Geological Survey: Jeddah, Saudi Arabia, 2002.
32. Kurdi, H.H. Geology and Resources of Basalt Quarry site Kishb-13, Southern Harrat Kishb. In *Open File Report SGSOF-2002-4*; Saudi Geological Survey: Jeddah, Saudi Arabia, 2002.
33. Khan, K.; Amin, M.N.; Saleem, M.U.; Qureshi, H.J.; Al-Faiad, M.A.; Qadir, M.G. Effect of Fineness of Basaltic Volcanic Ash on Pozzolanic Reactivity, ASR Expansion and Drying Shrinkage of Blended Cement Mortars. *Materials* **2019**, *12*, 2603. [CrossRef]
34. Khan, K.; Amin, M.N. Influence of fineness of volcanic ash and its blends with quarry dust and slag on compressive strength of mortar under different curing temperatures. *Constr. Build. Mater.* **2017**, *154*, 514–528. [CrossRef]
35. Moufti, M.R.; Sabtan, A.A.; El-Mahdy, O.R.; Shehata, W.M. Assessment of the industrial utilization of scoria materials in central Harrat Rahat, Kingdom of Saudi Arabia. *Eng. Geol.* **2000**, *57*, 155–162. [CrossRef]
36. Sabtan, A.A.; Shehata, W.M. Evaluation of engineering properties of scoria in central Harrat Rahat, Kingdom of Saudi Arabia. *Bull. Eng. Geol. Env.* **2000**, *59*, 219–225. [CrossRef]
37. Khan, M.I.; Alhozaimy, A.M. Properties of natural pozzolan and its potential utilization in environmental friendly concrete. *Can. J. Civ. Eng.* **2011**, *38*, 71–78. [CrossRef]
38. Al-Chaar, G.K.; Alkadi, M.; Asteris, P.G. Natural pozzolan as a partial substitute for cement in concrete. *Open Constr. Build. Technol. J.* **2013**, *7*, 33–42. [CrossRef]
39. Celik, K.; Jackson, M.D.; Mancio, M.; Meral, C.; Emwas, A.-H.; Mehta, P.K.; Monteiro, P.J.M. High-volume natural volcanic pozzolan and limestone powder as partial replacements for portland cement in self-compacting and sustainable concrete. *Cem. Concr. Compos.* **2014**, *45*, 136–147. [CrossRef]
40. Kupwade-Patil, K.; Al-Aibani, A.F.; Abdulsalam, M.F.; Mao, C.; Bumajdad, A.; Palkovic, S.D.; Buyukozturk, O. Microstructure of cement paste with natural pozzolanic volcanic ash and Portland cement at different stages of curing. *Constr. Build. Mater.* **2016**, *113*, 423–441. [CrossRef]
41. Letelier, V.; Ortega, J.M.; Tremiño, R.M.; Henriquéz-Jara, B.I.; Fustos, I.; Real-Herraiz, T.; Moriconi, G.; Climent, M.Á.; Sánchez, I. The Use of Volcanic Powder as a Cement Replacement for the Development of Sustainable Mortars. *Appl. Sci.* **2020**, *10*, 1460. [CrossRef]
42. Al-Fadala, J.S.; Chakkamalayath, S.; Al-Bahar, A.; Al-Aibani, S. Ahmed. Significance of performance based specifications in the qualification and characterization of blended cement using volcanic ash. *Constr. Build. Mater.* **2017**, *144*, 532–540. [CrossRef]

43. Charkhi, A.; Kazemian, H.; Kazemeini, M. Optimized experimental design for natural clinoptilolite zeolite ball milling to produce nano powders. *Powder Technol.* **2010**, *203*, 389–396. [CrossRef]
44. Usman, M.; Zhu, J.; Chuiyang, K.; Arslan, M.T.; Khan, A.; Galadima, A.; Muraza, O. Propene Adsorption-Chemisorption Behaviors on H-SAPO-34 Zeolite Catalysts at Different Temperatures. *Catalysts* **2019**, *9*, 919. [CrossRef]
45. Saamiya, S.; Raissa, D.F.; Maria, C.G.J. Calcining natural zeolites to improve their effect on cementitious mixture workability. *Cem. Concr. Res.* **2016**, *85*, 102–110.
46. Moussa, H.; Larbi, K.; Martin, C.; Pierre, C. Evaluation and improvement of pozzolanic activity of andesite for its use in eco-efficient cement. *Constr. Build. Mater.* **2013**, *47*, 1268–1277.
47. Kucukyıldırım, E.; Uzal, B. Characteristics of calcined natural zeolites for use in high-performance pozzolan blended cements. *Constr. Build. Mater.* **2014**, *73*, 229–234. [CrossRef]
48. Alaettin, K.; Zeynep, S. Effect of heat treatment on pozzolanic activity of volcanic pumice used as cementitious material. *Cem. Concr. Compos.* **2015**, *57*, 128–132.
49. Burris, L.E.; Juenger, M.C.G. Milling as a pretreatment method for increasing the reactivity of natural zeolites for use as supplementary cementitious materials. *Cem. Concr. Compos.* **2016**, *65*, 163–170. [CrossRef]
50. American Society for Testing and Materials. *Standard Specification for Portland Cement*. Available online: www.astm.org (accessed on 10 January 2022).
51. Methods of Testing Cement—Part 1: Determination of Strength. European Committee for Standardization. Available online: https://standards.cen.eu. (accessed on 10 January 2022).
52. Cement—Test Methods—Determination of Strength. International Organization for Standardization: Geneva, Switzerland, 2009. Available online: https://www.iso.org/standard/45568.html. (accessed on 10 January 2022).
53. American Society for Testing and Materials. *Standard Terminology Relating to Concrete and Concrete Aggregates*. Available online: www.astm.org (accessed on 10 January 2022).
54. American Society for Testing and Materials. *Standard Test Method for Compressive Strength of Hydraulic Cement Mortars (Using 2-in or 50-mm. Cube Specimens)*. Available online: www.astm.org (accessed on 10 January 2022).
55. Standard Practice for Mechanical Mixing of Hydraulic Cement Pastes and Mortars of Plastic Consistency. ASTM International: West Conshohocken, PA, USA, 2014. Available online: www.astm.org (accessed on 10 January 2022).
56. Standard Test Method for Dry and Wet Bulk Density, Water Absorption, and Apparent Porosity of Thin Sections of Glass-Fiber Reinforced Concrete. Available online: www.astm.org (accessed on 10 January 2022). [CrossRef]
57. Standard Specification for Coal Fly Ash and Raw or Calcined Natural Pozzolan for Use in Concrete. Available online: http://www.astm.org (accessed on 10 January 2022).
58. Beleuk à Moungam, L.M.; Lemougna, P.N.; Kaze, R.C.; Mohamed, H.; Deutou Nemaleu, J.G.; Billong, N.; Kamseu, E.; Mvondo-Ze, A.D.; Kenfack, I.T. Synthesis of Volcanic Ash-based Porous Inorganic Polymers Using Biomass as Pore Inducing Agent: Phase Evolution and Descriptive Microstructure. *Silicon* **2021**, 1–14. [CrossRef]
59. Metekong, J.V.S.; Kaze, C.R.; Deutou, J.G.; Venyite, P.; Nana, A.; Kamseu, E.; Melo, U.C.; Tatietse, T.T. Evaluation of performances of volcanic-ash-laterite based blended geopolymer concretes: Mechanical properties and durability. *J. Build. Eng.* **2020**, *34*, 101935. [CrossRef]
60. Kim, J.; Yi, C.; Zi, G. Waste glass sludge as a partial cement replacement in mortar. *Constr. Build. Mater.* **2015**, *75*, 242–246. [CrossRef]
61. Chindaprasirt, P.; Jaturapitakkul, C.; Sinsiri, T. Effect of fly ash fineness on microstructure of blended cement paste. *Constr. Build. Mater.* **2007**, *21*, 1534–1541. [CrossRef]
62. Altwair, N.M.; Azmi, M.; Johari, M.; Fuad, S.; Hashim, S. Strength activity index and microstructural characteristics of treated palm oil fuel ash. *Int. J. Civil Environ. Eng.* **2011**, *11*, 100–107.
63. Helmi, M.; Hall, M.R.; Stevens, L.A.; Rigby, S.P. Effects of high-pressure/temperature curing on reactive powder concrete microstructure formation. *Constr. Build. Mater.* **2016**, *105*, 554–562. [CrossRef]
64. Scrivener, K.; Snellings, R.; Lothenbach, B. *A Practical Guide to Microstructural Analysis of Cementitious Materials*; CRC Press: Boca Raton, FL, USA, 2016.
65. Yu, P.; Kirkpatrick, R.J.; Poe, B.; McMillan, P.F.; Cong, X. Structure of calcium silicate hydrate (C–S–H): Near-, Mid-, and Far-infrared spectroscopy. *J. Am. Ceram. Soc.* **1999**, *82*, 742–748. [CrossRef]
66. Hughes, T.L.; Methven, C.M.; Jones, T.G.; Pelham, S.E.; Fletcher, P.; Hall, C. Determining cement composition by Fourier transform infrared spectroscopy. *Adv. Cem. Based Mater.* **1995**, *2*, 91–104. [CrossRef]